Theory of a strained *p*-Ge resonant-state terahertz laser

M. A. Odnoblyudov,[1,2] A. A. Prokofiev,[1] I. N. Yassievich,[1,2] and K. A. Chao[2]
[1]*A. F. Ioffe Physico-Technical Institute, Russian Academy of Science, 194021 St. Petersburg, Russia*
[2]*Division of Solid State Theory, Department of Physics, Lund University, S-223 62 Lund, Sweden*
(Received 15 January 2004; published 21 September 2004)

A theory of a strained *p*-Ge resonant-state THz laser is developed. A comprehensive study of the processes leading to the stimulated THz emission in strained *p*-Ge under an electric field applied is presented. The distribution functions of light and heavy holes are found. The scattering by optical and acoustic phonons, as well as resonant scattering by charged impurities are taken into account. The steady-state hole distribution functions are used to calculate the generation-recombination coefficients which enter into the system of rate equations for the localized states populations. The populations of localized and resonant acceptor states are found. The conditions for population inversion are investigated. The optical gain calculation is carried out taking into account main optical transitions in the THz spectrum range.

DOI: 10.1103/PhysRevB.70.115209 PACS number(s): 78.67.De, 73.21.Fg, 73.20.Hb

I. INTRODUCTION

The spectral region between 1 and 20 THz remains the area of intensive research during the last two decades. THz radiation delivers important information on processes in solids, outerspace, biological objects, and can be used for medical imaging.[1–4] Up to very recent, available sources of the THz radiation included CO_2-pumped molecular or Raman gas lasers,[5] free electron lasers, backward-wave oscillators (BWO's), and Schottky diode multipliers,[6] *p*-Ge hot-hole lasers under simultaneously applied electric and magnetic fields.[7,8] Another approach for generation of the pulsed THz radiation was based on ultrafast carrier and phonon relaxation in semiconductors and superconductors, as well as in nonlinear crystals under intensive femtosecond excitation.[9–11] Some attempts were made to utilize nonlinear photomixing of two infrared or optical pulses.[12,13] All these sources were either technically complicated or limited in power. Moreover, main part of them could not produce tunable coherent cw radiation at frequencies above 1.5 THz. Thus, many possible applications of the THz radiation have been hampered by the lack of compact, low-consumption, tunable, solid-state terahertz sources.

Recently, the activity towards the quantum cascade THz laser (QCL) on the basis of SiGe/Si and III-V heterostructures has been started[14–18] and AlGaAs/GaAs QC THz laser has been fabricated.[19]

Very promising from an application point of view is the strained *p*-Ge THz laser,[20] which gives possibility to tune THz emission wavelength by applied stress. Breakthrough in the development of such a source is related with demonstration of the first widely tunable cw strained *p*-Ge THz laser.[21] In result of this work, a new type of solid state lasers, namely, a resonant-state laser (RSL), has been developed. The mechanism of operation of the strained *p*-Ge resonant-state laser is the following. In strained *p*-Ge the valence band top, as well as acceptor levels, are split. At sufficiently large stress, the level split off from the ground state enters the continuum of the valence band and becomes resonant. In an external electric field, localized states are depopulated due to impact ionization, while the resonant states are filled by holes due to coupling with the states of the valence band continuum. As a result, the intracenter population inversion can be formed and the THz stimulated emission occurs via optical transitions between the resonant and localized acceptor states. The idea of the resonant-state laser can be realized in a variety of systems. For example, in lattice mismatched $Si/Si_{1-x}Ge_x/Si$ quantum wells delta doped with boron the combined effect of confinement and internal strain results in the splitting of the acceptor levels and formation of acceptor resonant states, similar to those in strained *p*-Ge. Recently, a SiGe single QW resonant-state laser has also been realized.[22,23] Despite the lower power of the emission of the SiGe RSL in comparison with the AlGaAs/GaAs QCL, one should take into account that the active region of the RSL in Ref. 22 consists of only one QW and the structure itself is much simpler to fabricate.

The mechanism of operation of the *p*-Ge RSL is schematically shown in Fig. 1. Processes, which should be studied to understand the laser operation, are the resonant state formation, hole transport and resonant state population, impact ionization of the localized acceptor states and their populations, rates of possible optical transitions with energies in the THz range. Several theoretical papers were devoted to the analysis of the strained *p*-Ge RSL. The formation of acceptor resonant states and their characteristics such as energy position, lifetime, resonant scattering, and capture amplitudes were studied.[24–26] Transport of free holes in an external electric field in the presence of the resonant scattering was considered and hole distribution function and resonant state population was calculated in Ref. 27 However, no calculations of the impact ionization rates, the localized state populations and the optical gain in the THz frequency range have been performed so far to eventually proof that THz lasing is possible from such a system. In this paper we present an extended theoretical analysis of the strained *p*-Ge RSL.

 ©2004 The American Physical Society

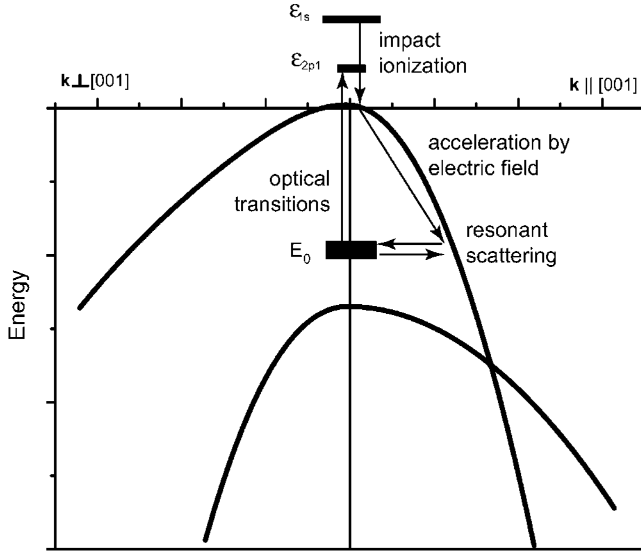

FIG. 1. The mechanism of operation of the *p*-Ge RSL

Background information about valence band in strained semiconductors and the resonant acceptor states is given in Sec. II and Appendix A. The distribution function of the light and heavy holes in the presence of the electric field will be found in Sec. III as a solution to Boltzmann equation. The effect of scattering of holes by optical and acoustic phonons, as well as the resonant scattering by impurity states will be included into the calculations. Then, in Sec. IV a consideration of impact ionization of the localized acceptor states by the electric field will be done to find both, the resonant states and localized states steady state populations, and to clear out conditions (electric field and stress values) for the formation of the intracenter population inversion. Steady state population of the localized acceptor states is established in result of exchange by holes between localized acceptor and valence band states, therefore the population depends on the distribution function of holes in the valence band. However, the steady state distribution of the light and heavy holes is formed during the time much shorter than the time of the formation of the steady state population of the localized states.[28] Therefore, the steady state hole distribution function found in Sec. III will be used to calculate generation-recombination (GR) coefficients, which appear in the rate equations for the localized states populations. These rate equations will include processes of thermal capture of holes by the localized impurity states, thermal emission of holes from the localized impurity states, processes of impact ionization of the localized states by free holes, and reverse Auger processes. Finally in Sec. V calculation of optical gain will be carried out, taking into account main optical transitions with energies in THz spectrum range. The paper could serve as a guidance for optimization of the strained *p*-Ge RSL THz laser and for development of another types of RSL's.

II. VALENCE BAND OF STRAINED CUBIC SEMICONDUCTORS AND ACCEPTOR RESONANT STATES

In terms of the Bloch basis $u_{\pm 3/2,\pm 1/2}$ of Γ_8^+ irreducible representation of the double point group $\bar{O}_h$, the Luttinger Hamiltonian operator describing the valence band states under an uniaxial stress P along z axis (parallel to [001] crystal axis) has the form

$$\hat{H}_{\mathrm{L}}(\hat{\mathbf{k}},\zeta)=\frac{\hbar^2}{2m_0}\begin{bmatrix}\hat{a}_+-2\gamma_1\zeta & \hat{b} & \hat{c} & 0\\ \hat{b}^* & \hat{a}_- & 0 & \hat{c}\\ \hat{c}^* & 0 & \hat{a}_- & -\hat{b}\\ 0 & \hat{c}^* & -\hat{b}^* & \hat{a}_+-2\gamma_1\zeta\end{bmatrix} \tag{1}$$

with the matrix elements

$$\hat{a}_+=-(\gamma_1-2\gamma_2)\hat{k}_z^2-(\gamma_1+\gamma_2)(\hat{k}_x^2+\hat{k}_y^2),$$

$$\hat{a}_-=-(\gamma_1+2\gamma_2)\hat{k}_z^2-(\gamma_1-\gamma_2)(\hat{k}_x^2+\hat{k}_y^2),$$

$$\hat{b}=2\sqrt{3}\gamma_3(\hat{k}_x-i\hat{k}_y)\hat{k}_z,$$

$$\hat{c}=0.5\sqrt{3}(\gamma_2+\gamma_3)(\hat{k}_x-i\hat{k}_y)^2, \tag{2}$$

where $\gamma_1=13.38, \gamma_2=4.24, \gamma_3=5.69$ are the Luttinger parameters, and ζ is related to the split of the valence band top E_{def} and to the deformation potential α_d by $E_{\mathrm{def}}=\alpha_d P=\hbar^2\zeta\gamma_1/m_0$. For Ge stressed along [001] axis, α_d equals to 5.5 meV/kbar. Here $\hat{\mathbf{k}}$ is the momentum operator. We have adopted cylindrical approximation for the Luttinger Hamiltonian.

The energy spectrum of the valence band of strained Ge and corresponding eigenfunctions in the Γ_8^+ basis are given by

$$\varepsilon_{\mathbf{k}}^{l,h}=-\frac{\hbar^2}{2m_0}[\gamma_1\zeta+\gamma_1(k_\perp^2+k_z^2)\mp\sqrt{\gamma_1^2\zeta^2+2\gamma_1\gamma_2\zeta(k_\perp^2-2k_z^2)+(\gamma_2^2+3\gamma_c^2)k_\perp^4+4\gamma_2^2k_z^4-4(\gamma_2^2-3\gamma_c^2)k_\perp^2k_z^2}] \tag{3}$$

and

$$\psi_{\mathbf{k}}^{l,+1/2}=\frac{1}{N_l}\frac{e^{i\mathbf{kr}}}{\sqrt{V}}\begin{bmatrix}-b\\ d_+^l\\ 0\\ -c^*\end{bmatrix},\quad \psi_{\mathbf{k}}^{l,-1/2}=\frac{1}{N_l}\frac{e^{i\mathbf{kr}}}{\sqrt{V}}\begin{bmatrix}-c\\ 0\\ d_+^l\\ b^*\end{bmatrix},$$

$$\psi_{\mathbf{k}}^{h,+3/2}=\frac{1}{N_h}\frac{e^{i\mathbf{kr}}}{\sqrt{V}}\begin{bmatrix}d_-^h\\ -b^*\\ -c^*\\ 0\end{bmatrix},\quad \psi_{\mathbf{k}}^{h,-3/2}=\frac{1}{N_h}\frac{e^{i\mathbf{kr}}}{\sqrt{V}}\begin{bmatrix}0\\ -c\\ b\\ d_-^h\end{bmatrix},$$

$$d_+^l=a_+-\frac{2m_0\varepsilon_{\mathbf{k}}^l}{\hbar^2}-2\gamma_1\zeta,\quad d_-^h=a_--\frac{2m_0\varepsilon_{\mathbf{k}}^h}{\hbar^2},$$

$$N_l^2=|b|^2+|c|^2+|d_+^l|^2,$$

$$N_h^2=|b|^2+|c|^2+|d_-^h|^2. \tag{4}$$

The energy of holes is counted from the top of the LH band, according to Fig. 1.

In the presence of a charged acceptor, one should complete the Luttinger Hamiltonian with the Coulomb potential term

$$V_c(\mathbf{r})=-\frac{e^2}{\kappa r}\hat{I}, \tag{5}$$

where e is the electron charge, κ is the dielectric constant, and $\hat{I}$ is the unit matrix. An approximation for the localized impurity states attached to the light hole band, as well as for the localized part of the resonant states, attached to the heavy hole band, can be obtain as an eigensolution to the Schrödinger equation

$$[\hat{H}_L^d+V_c(\mathbf{r})]\phi(\mathbf{r})=\varepsilon\phi(\mathbf{r}), \tag{6}$$

where $\hat{H}_L^d$ is the diagonal part of the Luttinger Hamiltonian in Eq. (1). This approximation corresponds to the high stress limit, when the light and the heavy hole bands are effectively decoupled.[24,31] In this limit, the localized states attached to the light hole band can be characterized by the total angular momentum projection at the Γ point equal to $m=\pm 1/2$, and those attached to the heavy hole band by $m=\pm 3/2$. In addition, these states are characterized by the projection of the orbital angular momentum l_z and parity i. As wave functions of the ground $(1s)$ localized state characterized by $m=+1/2, l_z=0, i=+1$ and the uppest (see Fig. 1) $(1s,\text{res})$ resonant state characterized by $m=+3/2$, $l_z=0, i=+1$ we adopt the most commonly used variational functions[32]

$$\varphi_{1s,\text{res}}^{+3/2}(\mathbf{r})=\frac{1}{\sqrt{\pi a^2 b}}\exp^{-\sqrt{\rho^2/a_{\text{res}}^2+z^2/b_{\text{res}}^2}}\begin{bmatrix}1\\0\\0\\0\end{bmatrix},$$

TABLE I. Energies and variational parameters for localized and resonant states.

Level	Energy, meV	Variational parameters, Å
$1s$	4.22	$a=95.0$, $b=13.0$
$2p1$	1.19	$c=178.0$, $d=235$
$1s,\text{res}$	4.37	$a_{\text{res}}=117.0$, $b_{\text{res}}=74.9$

$$\varphi_{1s}^{+1/2}(\mathbf{r})=\frac{1}{\sqrt{\pi a^2 b}}\exp^{-\sqrt{\rho^2/a^2+z^2/b^2}}\begin{bmatrix}0\\1\\0\\0\end{bmatrix}. \tag{7}$$

As a wave function of the first excited $(2p1)$ localized state, characterized by $m=+1/2, l_z=\pm 1, i=+1$, we adopt the following variational function:

$$\varphi_{2p1}^{+1/2}(\mathbf{r})=\frac{1}{\sqrt{\pi c^4 d}}\rho e^{\pm i\phi}\exp^{-\sqrt{\rho^2/c^2+z^2/d^2}}\begin{bmatrix}0\\1\\0\\0\end{bmatrix}. \tag{8}$$

The index $m=+3/2,+1/2$ shows here which of the Γ_8^+ basis states gives contribution to the impurity state wave function. The parameters of the wave functions $a_{\text{res}}, b_{\text{res}}, a, b, c, d$ and the corresponding energies of the states are found from variational solution of Eq. (6) and are given in Table I. The energies ε_{1s}, ε_{2p1}, and $\varepsilon_{1s,\text{res}}$ are measured from the extrema of the light and heavy hole bands, correspondingly. Note, that all the energy levels have additional twofold degeneracy in respect to the sign of m.

We construct the resonant state wave function in the form

$$\Psi_{\mathbf{k}}^{+1/2}=\psi_{\mathbf{k}}^{+1/2}+\sum_{m=\pm 3/2}a_{\mathbf{k}}^{+1/2,m}\varphi_{1s,\text{res}}^{m}(\mathbf{r})+\sum_{\mathbf{k}',m'=\pm 1/2}\frac{t_{\mathbf{kk}'}^{+1/2,m'}}{\varepsilon_{\mathbf{k}}^l-\varepsilon_{\mathbf{k}'}^l+i\gamma}\psi_{\mathbf{k}'}^{m'}(\mathbf{r}), \tag{9}$$

where $\gamma\to 0$. Capture and scattering amplitudes entering into Eq. (9) were derived in Ref. 26 using combined Fano-Dirac approach and are given by the equations

$$a_{\mathbf{k}}^{+1/2,m}=\frac{1}{\sqrt{V}}\frac{1}{\varepsilon_{\mathbf{k}}^l-(\varepsilon_{1s,\text{res}}-E_{\text{def}}+\Delta E_{\mathbf{k}})+i\Gamma/2}A_{\mathbf{k}}^{+1/2,m}, \tag{10}$$

$$t_{\mathbf{k}\cdot\mathbf{k}'}^{+1/2,+1/2}=-\frac{\tilde{V}_{\mathbf{k}'\mathbf{k}}^{+1/2,+1/2}}{V}-\frac{W_{\mathbf{k}'}}{\sqrt{V}}\frac{\hbar^2}{2m_0}\frac{d_+^l}{N_l(\mathbf{k}')}[b^*(\mathbf{k}')a_{\mathbf{k}}^{+1/2,+3/2}+c(\mathbf{k}')a_{\mathbf{k}}^{+1/2,-3/2}],$$

$$t_{\mathbf{k}\cdot\mathbf{k}'}^{+1/2,-1/2} = -\frac{\widetilde{V}_{\mathbf{k}'\mathbf{k}}^{-1/2,+1/2}}{V} - \frac{W_{\mathbf{k}'}}{\sqrt{V}}\frac{\hbar^2}{2m_0}\frac{d_+}{N_l(\mathbf{k}')}[c^*(\mathbf{k}')a_{\mathbf{k}}^{+1/2,+3/2} - b(\mathbf{k}')a_{\mathbf{k}}^{+1/2,-3/2}]. \quad (11)$$

Expression for $A_{\mathbf{k}}^{+1/2,m}$ and for the matrix elements are given in Appendix A. Expressions for $\Delta E_{\mathbf{k}}$ and $\Gamma_{\mathbf{k}}$ have been derived in Ref. 26. The first terms in the expressions (11) for $t_{\mathbf{k}\mathbf{k}'}^{m,m'}$ describe elastic scattering by ionized impurities in Born approximation. One can see from Eq. (10) that the hybridization of the continuum light hole states and the resonant $(1s,\text{res})$ state results in the shift of the resonance position from $\varepsilon_{1s,\text{res}}$ by $\Delta E_{\mathbf{k}}$, which is a function of $\mathbf{k}$. $\Gamma_{\mathbf{k}}$ has meaning of the resonance width. The energy E_0 of the impurity induced resonance in the light hole band can be defined as a solution to the equation

$$E_0 + E_{\text{def}} - \varepsilon_{1s,\text{res}} - \Delta E(E_0) = 0. \quad (12)$$

The results of such procedure were presented in Ref. 26. Then, one can take the value of the $\Gamma_{\mathbf{k}}$ at the resonance energy E_0 as the resonance width.

Probabilities of capture into the resonant state and elastic resonant scattering are given by the equations[26]

$$W_{\mathbf{k}r} = |a_{\mathbf{k}}^{+1/2,+3/2}|^2 + |a_{\mathbf{k}}^{+1/2,-3/2}|^2,$$

$$W_{\mathbf{k}\cdot\mathbf{k}'}^{\text{res}} = \frac{2\pi}{\hbar}(|t_{\text{res},\mathbf{k}\cdot\mathbf{k}'}^{+1/2,+1/2}|^2 + |t_{\text{res},\mathbf{k}\cdot\mathbf{k}'}^{+1/2,-1/2}|^2)\delta(\varepsilon_{\mathbf{k}}^l - \varepsilon_{\mathbf{k}'}^l), \quad (13)$$

where $t_{\text{res},\mathbf{k}\cdot\mathbf{k}'}^{m,m'}$ are the resonant scattering amplitudes given by the second terms of $t_{\mathbf{k}\cdot\mathbf{k}'}^{m,m'}$ [see Eq. (11)]. The probabilities in Eq. (13) can be presented in the form

$$W_{\mathbf{k}r} = \frac{16\pi a_{\text{res}}^2 b_{\text{res}}}{V}\frac{\left(\frac{e^2}{\kappa_0 a_{\text{res}}}\right)^2}{(\varepsilon_{\mathbf{k}}^l - E_0)^2 + \Gamma^2/4}w(\mathbf{k}),$$

$$W_{\mathbf{k}\cdot\mathbf{k}'}^{\text{res}} = \frac{2\pi}{\hbar}\frac{2^{10}(\pi a_{\text{res}}^2 b_{\text{res}})^2}{V^2}\frac{\hbar^4}{4m_0^2 a_{\text{res}}^4}\widetilde{w}(\mathbf{k})\,\eta(\mathbf{k}') \times \frac{\left(\frac{e^2}{\kappa_0 a_{\text{res}}}\right)^2}{(\varepsilon_{\mathbf{k}}^l - E_0)^2 + \Gamma^2/4}\delta(\varepsilon_{\mathbf{k}}^l - \varepsilon_{\mathbf{k}'}^l), \quad (14)$$

where $w(\mathbf{k})$, $\widetilde{w}(\mathbf{k})$, and $\eta(\mathbf{k}')$ are dimensionless functions which describe angular dependencies of the probabilities. These functions are given by

$$w(\mathbf{k}) = \frac{\left(\frac{e^2}{\kappa_0 a_{\text{res}}}\right)^{-2}}{16\pi a_{\text{res}}^2 b_{\text{res}}}(|A_{\mathbf{k}}^{+1/2,+1/2}| + |A_{\mathbf{k}}^{+1/2,-1/2}|)^2,$$

$$\widetilde{w}(\mathbf{k}) = w(\mathbf{k})(a_{\text{res}}^2 d_+^l)^2,$$

$$\eta(\mathbf{k}') = \frac{|b(\mathbf{k}')|^2 + |c(\mathbf{k}')|^2}{N_l^2(\mathbf{k}')}\frac{1}{[1 + (k_z' b_{\text{res}})^2 + (k_\perp' a_{\text{res}})^2]^2} \quad (15)$$

and are shown in Fig. 2. From Fig. 2(a) one can see that the capture into the resonant state is absent when perpendicular to the z axis component of the hole momentum is zero, i.e., when the hole moves along the stress axis. In this case, hole states in the light hole band [Eq. (4)] have no contribution from the basis states $u_{\pm 3/2}$ and cannot be coupled with the resonant states $\varphi_{1s,\text{res}}^{\pm 3/2}(\mathbf{r})$. One should mention that the complete expressions for the scattering amplitudes in Eq. (10) includes also scattering by ionized acceptors in addition to the resonant scattering. Thus, the total scattering probability $W_{\mathbf{k}\cdot\mathbf{k}'}$ obtained from the $t_{\mathbf{k}\cdot\mathbf{k}'}^{m,m'}$ in a way similar to Eq. (13) also includes both types of impurity scattering.

III. KINETICS OF HOLES IN THE VALENCE BAND

In general, behavior of holes in the presence of an external electric field E directed along z axis should be described within the density matrix formalism $\rho_{\mathbf{k}}^{mm'}$, because of strong spin-orbit interaction, which results in mixing of the degenerate valence band states. However, it was shown in Ref. 25, that the equation for the density matrix can be reduced to the Boltzmann kinetic equations for the sum of diagonal elements of the density matrix

$$f_{\mathbf{k}}^l = \rho_{\mathbf{k}}^{+1/2+1/2} + \rho_{\mathbf{k}}^{-1/2-1/2},$$

$$f_{\mathbf{k}}^h = \rho_{\mathbf{k}}^{+3/2+3/2} + \rho_{\mathbf{k}}^{-3/2-3/2}, \quad (16)$$

which give the total population of both degenerate states in each band at given $\mathbf{k}$. It was also derived in Ref. 25 that in Born approximation the scattering term in the equation for the density matrix can be converted into the standard collision integral, which involves the distribution functions defined by Eq. (16). This is also valid for the resonant impurity scattering, which appears beyond the Born approximation, provided that the concentration of scattering centers is low enough to consider each scattering event independently. Thus, in the presence of an external electric field directed along the z axis, both acoustic and optical phonon scattering, as well as resonant impurity scattering, the total occupation probabilities of the light $f_{\mathbf{k}}^l$ and heavy $f_{\mathbf{k}}^h$ hole band states should be found from the following coupled Boltzmann kinetic equations:

$$\frac{e\mathcal{E}}{\hbar}\frac{\partial f_{\mathbf{k}}^\lambda}{\partial k_z} = \left(VN_A\sum_{\mathbf{k}'} W_{l\mathbf{k},l\mathbf{k}'}f_{\mathbf{k}'}^l - VN_A f_{\mathbf{k}}^l\sum_{\mathbf{k}'} W_{l\mathbf{k}',l\mathbf{k}}\right)\delta_{\lambda,l} + \sum_{\lambda'=l,h;\mathbf{k}'} f_{\mathbf{k}'}^{\lambda'}W_{\lambda\mathbf{k},\lambda'\mathbf{k}'}^{\mu,\pm} - f_{\mathbf{k}}^\lambda\sum_{\lambda'=l,h;\mathbf{k}'} W_{\lambda'\mathbf{k}',\lambda\mathbf{k}}^{\mu,\pm}, \quad (17)$$

where $\lambda=l,h$ denotes light and heavy hole bands, $\mu=\text{ac, opt}$ denotes scattering mechanisms, $W_{\lambda\mathbf{k},\lambda'\mathbf{k}'}^{\text{ac},\pm}$ is the probability of inelastic scattering with emission (+) and absorption (–) of acoustic phonons, $W_{\lambda\mathbf{k},\lambda'\mathbf{k}'}^{\text{opt}}$ is the probability of scattering due to emission of optical phonons, and N_A is the concentration of acceptors. $W_{l\mathbf{k},l\mathbf{k}'}$ are the full probabilities of elastic scattering. We have adopted the cylindrical approximation for the energy spectrum of the valence band, therefore the dispersion relations given by Eq. (3) depends

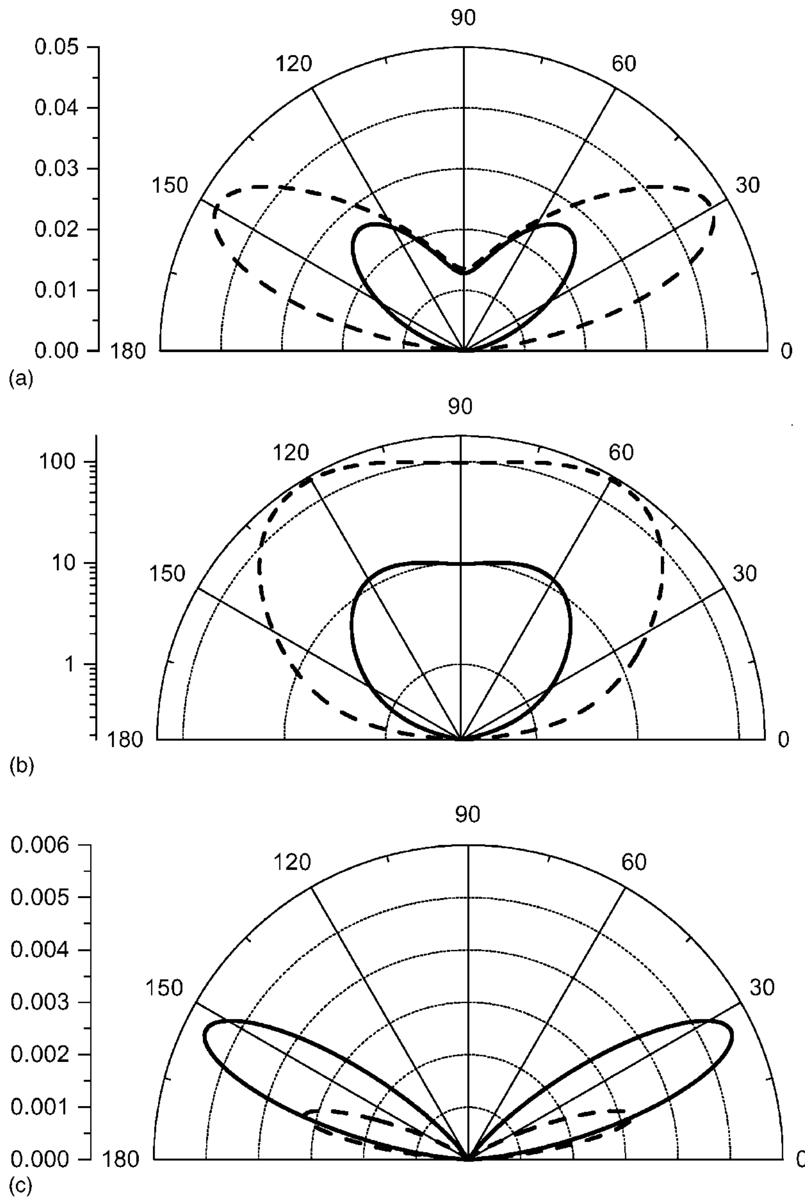

FIG. 2. (a) Angular dependence of the function $w(\mathbf{k})$. (b) Angular dependence of the function $\tilde{w}(\mathbf{k})$. (c) Angular dependence of the function $\eta(\mathbf{k}')$. Calculations are done for the stress values of 2 (solid line) and 4 kbar (dashed line). The value of $\mathbf{k}$ used to evaluate these functions at each angle of $\mathbf{k}$ corresponds to the resonance energy E_0 at given stress value.

only on k_z and $k_\perp = \sqrt{k_x^2 + k_y^2}$ components of the hole momentum in the coordinate system with z axis along the stress direction. Nevertheless, the distribution functions $f^{\lambda}_{\mathbf{k}}$, in general, depend on all three components of $\mathbf{k}$, because the probabilities of scattering due to interaction with acoustical phonons depend on the difference between polar angles ϕ and ϕ' of momenta $\mathbf{k}$ and $\mathbf{k}'$. To neglect dependencies of the distribution functions on the polar angles, we integrate the kinetic equations in Eq. (17) over ϕ, introducing average distribution functions

$$\bar{f}^{\lambda}_{k_z k_\perp} = \frac{1}{2\pi}\int_0^{2\pi} f^{\lambda}_{\mathbf{k}} d\phi, \tag{18}$$

which only depend on k_z and $k_\perp$. In result, the system of kinetic equations in Eq. (17) takes the form

$$\begin{aligned}\frac{e\mathcal{E}}{\hbar}\frac{\partial \bar{f}^{\lambda}_{k_z k_\perp}}{\partial k_z} = {}& \left(N_A \frac{V^2}{(2\pi)^2}\int\int k'_\perp dk'_\perp dk'_z \bar{W}_{l k_z k_\perp, l k'_z k'_\perp} \bar{f}^{l}_{k'_z k'_\perp} \right. \\ & \left. - N_A \frac{V^2}{(2\pi)^2}\bar{f}^{\lambda}_{k_z k_\perp}\int\int k'_\perp dk'_\perp dk'_z \bar{W}_{l k'_z k'_\perp, l k_z k_\perp}\right)\delta_{\lambda,l} \\ & + \frac{V}{(2\pi)^2}\sum_{\lambda'=l,h}\int\int k'_\perp dk'_\perp dk'_z \bar{W}^{\mu,\pm}_{\lambda k_z k_\perp, \lambda' k'_z k'_\perp}\bar{f}^{l}_{k'_z k'_\perp} \\ & - \bar{f}^{\lambda}_{k_z k_\perp}\frac{V}{(2\pi)^2}\sum_{\lambda'=l,h}\int\int k'_\perp dk'_\perp dk'_z \bar{W}^{\mu,\pm}_{\lambda k'_z k'_\perp, \lambda' k_z k_\perp},\end{aligned} \tag{19}$$

where $\bar{W}^{\mu,\pm}_{\lambda k_z k_\perp, \lambda' k'_z k'_\perp}$ are the scattering probabilities averaged either over ϕ or ϕ' scattering probabilities. Such averaging is possible due to dependence of the scattering probabilities only on the difference between ϕ and ϕ'. From now on we

skip the bar in Eq. (19) and denote the averaged distribution functions by $f_{\mathbf{k}}^{\lambda}$.

We define the population of the resonant state $f_r = f_r^{+1/2} + f_r^{-1/2}$ as the total probability to find a hole in the localized parts of the degenerated hybrodized states $\Psi_{\mathbf{k}}^{\pm 1/2}$, which is related with $f_{\mathbf{k}}^{l}$ (Refs. 26 and 27)

$$f_r = \sum_{\mathbf{k}} W_{\mathbf{k}r} f_{\mathbf{k}}^{l}, \tag{20}$$

where $W_{\mathbf{k}r}$ is the probability of capture into the resonant state given by Eq. (14). We assume that Ge sample is doped with Ga acceptors of concentration $N_A = 10^{14}$ cm^{-3} and contains compensating donor impurities of concentration $N_D = 10^{12}$ cm^{-3}. The distribution functions $f_{k_z k_\perp}^{l}, f_{k_z k_\perp}^{l}$ and the resonant state population f_r should satisfy the normalization condition

$$\frac{1}{V}\sum_{\mathbf{k}} f_{\mathbf{k}}^{l} + \frac{1}{V}\sum_{\mathbf{k}} f_{\mathbf{k}}^{h} + (N_D + p) f_r = p$$

or

$$p_l + p_h + (N_D + p) f_r = p, \tag{21}$$

where p is the concentration of holes in the valence band including holes populating resonant state, p_l and p_h are the concentrations of holes in the light and heavy hole bands, $N_D + p$ is the concentration of unpopulated acceptors, which can capture holes into the resonant states. At this stage the concentration p is unknown, because it depends on the populations of the localized states, which should be found from the system of rate equations. Therefore, we present distribution functions in the form

$$f_{\mathbf{k}}^{\lambda} = A \widetilde{f}_{\mathbf{k}}^{\lambda}, \tag{22}$$

where A is a normalization constant and $\widetilde{f}_{k_z k_\perp}^{\lambda}$ are normalized by the condition

$$\frac{1}{(2\pi)^3} \int d\widetilde{\mathbf{k}} (\widetilde{f}_{\mathbf{k}}^{l} + \widetilde{f}_{\mathbf{k}}^{h}) = N_l + N_h = 1. \tag{23}$$

Here we have introduced dimensionless momentum $\widetilde{\mathbf{k}} = \mathbf{k}/\alpha$, where $\alpha = \sqrt{2m_0 \hbar\omega_{\mathrm{opt}}/\gamma_1 \hbar^2}$ and $E_{\mathrm{opt}} = \hbar\omega_{\mathrm{opt}}$ is the optical phonon energy. Thus, the distribution functions $\widetilde{f}_{k_z k_\perp}^{\lambda}$ can be obtained from Eqs. (17) completed with the normalization condition in Eq. (23). When the kinetic equation is solved, the concentrations p_l and p_h are given by

$$p_l = \alpha^3 A N_l, \quad p_h = \alpha^3 A N_h. \tag{24}$$

From Eqs. (20) and (22) one can obtain normalized resonant state population $\widetilde{f}_r$

$$\widetilde{f}_r = \frac{V\alpha^3}{(2\pi)^3} \int d^3\widetilde{\mathbf{k}} W_{\mathbf{k}r} \widetilde{f}_{\mathbf{k}}^{l}. \tag{25}$$

Taking into account Eqs. (22), (23), and (25), the normalization condition Eq. (21) becomes

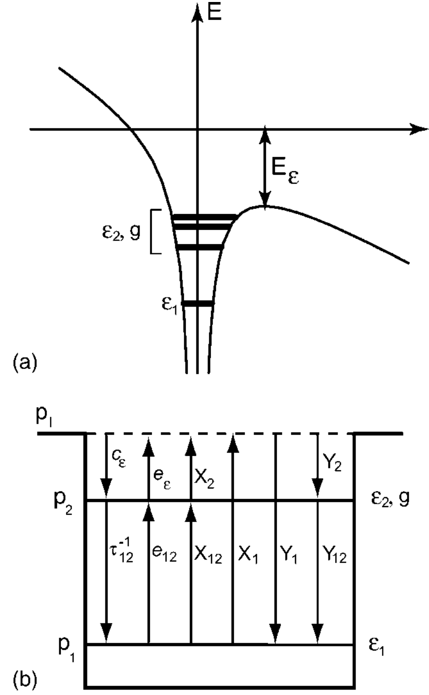

FIG. 3. (a) Coulombic impurity in an external electric field and the "two-level" model. (b) Schematic representation of the "two-level" model for the impurity level structure and processes determining populations of the levels 1 and 2.

$$\alpha^3 A + A(N_D + p)\widetilde{f}_r = p. \tag{26}$$

Using Eqs. (24) and (26), one can express p via p_l

$$p = p_l \frac{\alpha^3 + N_D \widetilde{f}_r}{\alpha^3 N_l - p_l \widetilde{f}_r}. \tag{27}$$

IV. LOCALIZED STATES POPULATION

The cw operation of the strained p-Ge THz laser was realized at electric field values below 10 V/cm, i.e., at voltages just above the impurity breakdown threshold. It was shown[28,29] that the "two-level model"[29] for impurity level structure should be used in order to describe adequately populations of the impurity levels and S shape of the current voltage characteristics in the breakdown and post-breakdown regimes. According to the model, we consider ground impurity level (1s) as a separate level with energy ε_1, but all the excited levels are combined into an effective level with energy ε_2 and degree of degeneracy g [see Fig. 3(a)]. For shallow acceptors the energy distances between the excited states are very small, therefore one can assume that all these states have the same population as the effective level with the energy ε_2. We also take into account Pool-Frenkel effect, i.e., the decrease of the impurity ionization potential by the amount $E_{\mathcal{E}} = 2(e^3\mathcal{E}/\kappa_0)^{1/2}$ [see Fig. 3(a)] in the external electric field $\mathcal{E}$. Thus, as the degree of degeneracy g we will take the number of excited Coulombic states with ionization energies larger than $E_{\mathcal{E}}$ multiplied by the degeneracy factor of

each level in respect to angular momentum. Let us introduce population functions of the ground $f_1=f_1^{+1/2}+f_1^{-1/2}$ and the excited $f_2=f_2^{+1/2}+f_2^{-1/2}$ states according to the relations

$$f_1 N_A = p_1, \quad f_2 N_A g = p_2, \tag{28}$$

where p_1 and p_2 are the concentrations of impurities with occupied ground and excited states, correspondingly. These functions also account for spin degeneracy.

The system of rate equations for the p_l, p_1, p_2 has the form[28]

$$\frac{dp_l}{dt} = -p_l(N_D+p)c_{\mathcal{E}} + p_2 e_{\mathcal{E}} + X_2 p_2 p_l - Y_2(N_D+p)p_l^2 + X_1 p_1 p_l - Y_1(N_D+p)p_l^2,$$

$$\frac{dp_2}{dt} = p_l(N_D+p)c_{\mathcal{E}} - e_{\mathcal{E}} p_2 - X_2 p_2 p_l + Y_2(N_D+p)p_l^2 + X_{12} p_l p_1 - Y_{21} p_l p_2 - \frac{p_2}{\tau_{12}} + e_{12} p_1,$$

$$N_A - N_D = p + p_1 + p_2, \tag{29}$$

where $c_{\mathcal{E}}$ is the capture coefficient to the energy level ε_2 in the presence of the electric field, $e_{\mathcal{E}}$ is the thermal emission coefficient from the energy level ε_2 in the presence of the electric field, e_{12} is the thermal emission coefficient from the ground into the excited impurity level, τ_{12}^{-1} defines the probability of the transition from the excited into the ground impurity level due to emission of acoustic phonon, X_1 and X_2 are the impact ionization coefficients from the ground and the excited impurity levels, correspondingly, X_{12} is the impact ionization coefficient from the ground into the excited impurity level [see Fig. 3(b)], and Y_1, Y_2, and Y_{12} are the coefficients of the reverse Auger processes. The last equation is the balance equation, which shows that the total hole concentration summed over the band and impurity states is equal to the number of uncompensated acceptors. At low values of the electric field, the concentration of light holes is much large than that of heavy holes, therefore we have assumed that only light holes contribute to the localized impurity states population. To calculate GR coefficients we will use a simplified model of the isotropic and parabolic light hole band with the effective mass equal to that of the density of states

$$m_\parallel = \frac{m_0}{\gamma_1 + 2\gamma_2}, \quad m_\perp = \frac{m_0}{\gamma_1 - \gamma_2}, \quad m = (m_\parallel m_\perp^2)^{1/3}, \tag{30}$$

where $m_\parallel$ and $m_\perp$ are the effective masses near the top of the light hole band parallel and perpendicular to the stress axis. Correspondingly, we assume the hydrogen level structure of the impurity center

$$\varepsilon_n = -\frac{E_B}{n^2}, \quad E_B = \frac{me^4}{2\hbar^2\kappa_0^2}, \tag{31}$$

Thus, we get

$$\varepsilon_1 = -4.34 \text{ meV},$$

$$\varepsilon_2 = -1.08 \text{ meV}. \tag{32}$$

The variational calculation of the energies of the localized acceptor states (see Table I) gives numbers which are very close to those obtained by Eq. (31).

A. Thermal emission and capture rates

For the thermal emission $e_{\mathcal{E}}$ and capture $c_{\mathcal{E}}$ rates we will use the expressions obtained within the "cascade capture model" (Ref. 30)

$$e_{\mathcal{E}} = e\left(1 + \frac{E_{\mathcal{E}}}{k_B T}0.98\right)^{-1} e^{E_{\mathcal{E}}/k_B T},$$

$$e = e^{-|\varepsilon_2|/k_B T}\frac{4m}{3\pi l_0 k_B T}\left(\frac{e^2}{\kappa_0\hbar}\right)^3, \tag{33}$$

and

$$c_{\mathcal{E}} = \frac{f^l_{k_z k_\perp}(k_z=0,k_\perp=0)}{p_l}\frac{4m}{3\pi l_0 k_B T}\left(\frac{e^2}{\kappa_0\hbar}\right)^3\left(1 + \frac{E_{\mathcal{E}}}{k_B T}0.98\right)^{-1}, \tag{34}$$

where $f^l_{k_z k_\perp}(k_z=0,k_\perp=0)$ is the value of the light-hole distribution function at the band top, l_0 is the effective length of hole–acoustic-phonon interaction

$$l_0 = \frac{\pi\hbar^4\rho}{2m^{5/2}m_c^{1/2}E_D^2}, \tag{35}$$

$m_c^{-1}=m_\parallel^{-1}/3+2m_\perp^{-1}/3$ is the conductivity effective mass, E_D is the deformation potential for hole–acoustic-phonon interaction, ρ is the crystal density, k_B is the Boltzmann constant, and T is the lattice temperature. The probability of the transition τ_{21}^{-1} between the excited ε_2 and ground ε_1 s-type impurity levels, accompanied by emission of acoustic phonon, is given by

$$\frac{1}{\tau_{21}} = \frac{s}{l_0}2^{10}\frac{ms^2}{E_B}\frac{n_1^7 n_2^7}{n_2^5 - n_1^5}, \tag{36}$$

where s is the velocity of sound, and $n_1=1, n_2=2$.

B. Impact ionization and auger coefficients

The impact ionization coefficient X_n from a level n is defined as[28]

$$X_n = \frac{1}{p_l}\frac{V}{(2\pi)^3}\int d\mathbf{k} W^i_{\mathbf{k},n} f^l_{\mathbf{k}}, \tag{37}$$

where $W^i_{\mathbf{k},n}$ is the probability of impact ionization of the nth impurity level by the electron with momentum $\mathbf{k}$. This probability is calculated in Appendix C [see Eq. (C6)] and is given by

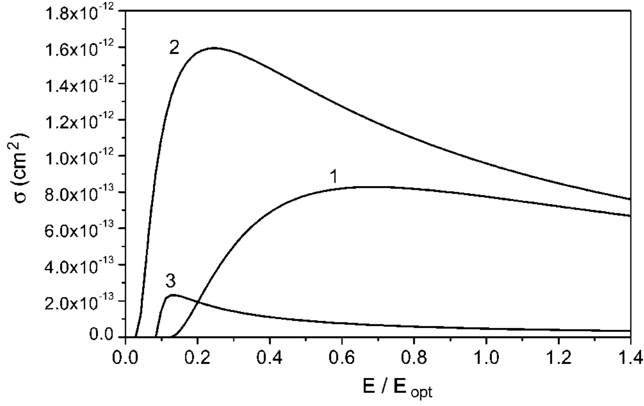

FIG. 4. Cross sections of the impact ionization from the level $n=1$ (curve 1), from the level $n=2$ (curve 2), from the level $n=1$ to the level $n=2$ (curve 3) as a function of hole kinetic energy.

$$W^i_{\mathbf{k},n} = 32\frac{a_B^3 n^3}{V}\frac{E_B}{\hbar}\mathcal{I}_1\left(\frac{\varepsilon_{\mathbf{k}}}{E_B}\right), \tag{38}$$

where the function $\mathcal{I}_1(\varepsilon_{\mathbf{k}}/E_B)$ is also derived in Appendix C. One can introduce the impact ionization cross section according to the definition (see Fig. 4)

$$W^i_{\mathbf{k},n} = \frac{1}{V}\frac{\hbar k}{m}\sigma^i_{\mathbf{k}}. \tag{39}$$

It gives for $\sigma^i_{\mathbf{k}}$ the following expression:

$$\sigma^i_{\mathbf{k}} = 16 a_B^2 n^3 \sqrt{\frac{E_B}{\varepsilon_{\mathbf{k}}}}\mathcal{I}_1\left(\frac{\varepsilon_{\mathbf{k}}}{E_B}\right). \tag{40}$$

Substitution of Eqs. (22), (38) into Eq. (37) gives the following expression for X_n:

$$X_n = \frac{A}{p_l}\frac{E_B}{\hbar}\frac{16n^3}{\pi^2}\int_{1/n^2}^{\infty} d\left(\frac{\varepsilon_{\mathbf{k}}}{E_B}\right)\int_0^{\pi} \sin\,\theta d\theta\sqrt{\frac{\varepsilon_{\mathbf{k}}}{E_B}}\tilde{f}_{\mathbf{k}'}\mathcal{I}_1\left(\frac{\varepsilon_{\mathbf{k}}}{E_B}\right). \tag{41}$$

Auger coefficients Y_n are introduced similar to Eq. (37)

$$Y_n = \frac{1}{p_l^2}\frac{V^2}{(2\pi)^6}\int d\mathbf{k}'\int d\mathbf{k}'' W^A_{\mathbf{k}',\mathbf{k}''} f^l_{\mathbf{k}'} f^l_{\mathbf{k}''}, \tag{42}$$

Here $W^A_{\mathbf{k}',\mathbf{k}''}$ is the Auger probability given by

$$W^A_{\mathbf{k}',\mathbf{k}''} = \frac{2\pi}{\hbar} g_n \sum_{\mathbf{k}} |M_{\mathbf{k}',\mathbf{k}'',\mathbf{k}}|^2 \delta(\varepsilon_{\mathbf{k}'} + \varepsilon_{\mathbf{k}''} - \varepsilon_{\mathbf{k}} + |\varepsilon_n|), \tag{43}$$

where $M_{\mathbf{k}',\mathbf{k}'',\mathbf{k}}$ is also given by Eq. (C2), g_n is the degeneracy factor of the level n. The impact ionization coefficient $X_{n_1n_2}$ from the level n_1 to the level n_2 is defined as

$$X_{n_1n_2} = \frac{1}{p_l}\frac{V}{(2\pi)^3}\int d\mathbf{k} W^i_{\mathbf{k},n_1,n_2} f^l_{\mathbf{k}}, \tag{44}$$

where $W^i_{\mathbf{k},n_1,n_2}$ is the probability of the corresponding process. Calculation of $W^i_{\mathbf{k},n_1,n_2}$ is carried out in Appendix C [see Eq. (C11)]. The cross section of this process is given by

$$\sigma^i_{\mathbf{k},n_1,n_2} = 2^9 \pi g_{n_2}\frac{\tilde{n}^6}{n_1^3 n_2^3} a_B^2 \sqrt{\frac{E_B}{\varepsilon_{\mathbf{k}}}}\sqrt{\varepsilon'} \times \mathcal{J}_1\left(\frac{\varepsilon_{\mathbf{k}}}{E_B},\varepsilon'\right). \tag{45}$$

Substituting Eq. (C11) into Eq. (44), the following expression for $X_{n_1n_2}$ is obtained:

$$X_{n_1n_2} = \frac{A}{p_l}\frac{E_B}{\hbar}\frac{2^7}{\pi} g_{n_2}\frac{\tilde{n}^6}{n_1^3 n_2^3} \times \int_{1/n_1^2-1/n_2^2}^{\infty}\int_0^{\pi} \sin\,\theta\, d\,\theta\, d\left(\frac{\varepsilon_{\mathbf{k}}}{E_B}\right)\sqrt{\frac{\varepsilon_{\mathbf{k}}}{E_B}}\sqrt{\varepsilon'} \times \mathcal{J}_1\left(\frac{\varepsilon_{\mathbf{k}}}{E_B},\varepsilon'\right)\tilde{f}_{k_z k_\perp}. \tag{46}$$

The coefficient for the reverse Auger process is defined as

$$Y_{n_1n_2} = \frac{1}{p_l}\frac{V}{(2\pi)^3}\int d\mathbf{k}' W^A_{\mathbf{k}',n_1,n_2} f^l_{\mathbf{k}'}. \tag{47}$$

The probability of this process can be obtained from Eq. (46) by replacing $\sqrt{\varepsilon'}$ by $\sqrt{\varepsilon_{\mathbf{k}}/E_B}$ and taking $\varepsilon_{\mathbf{k}}/E_B = \varepsilon' + n_1^{-2} - n_2^{-2}$. Then, the corresponding Auger coefficient becomes

$$Y_{n_1n_2} = \frac{A}{p_l}\frac{E_B}{\hbar}\frac{2^8}{\pi} g_{n_2}\frac{\tilde{n}^6}{n_1^3 n_2^3} \times \int_0^{\infty} d\varepsilon' \int_0^{\pi} \sin\,\theta\, d\,\theta \sqrt{\frac{\varepsilon_{\mathbf{k}}}{E_B}}\sqrt{\varepsilon'}\mathcal{J}_1\left(\frac{\varepsilon_{\mathbf{k}}}{E_B},\varepsilon'\right)\tilde{f}_{k_z k_\perp}, \tag{48}$$

$$\frac{\varepsilon_{\mathbf{k}}}{E_B} = \varepsilon' + \frac{1}{n_1^2} - \frac{1}{n_2^2}. \tag{49}$$

C. Solution of the rate equations

We are interested in a steady state solution of the system of rate equations Eq. (29). By putting time derivative terms equal to zero and combining three equations in Eq. (29) with the Eq. (27), we obtain a system of four equations for four unknown concentrations p, p_l, p_1, p_2. This system can be reduced to one equation for p_l

$$p_l^2(Y_1 + Y_2)(N_A - p_1 - p_2) - p_l[X_1 p_1 + X_2 p_2 - c_\varepsilon(N_A - p_1 - p_2)] - p_2 e_\varepsilon = 0, \tag{50}$$

where p_1, p_2, and p are functions of p_l

$$p_1 = \frac{Y_1(N_D + p)p_l^2 + (Y_{21}p_l + \tau_{12}^{-1})(N_A - N_D - p)}{p_l(X_1 + X_{12} + Y_{21}) + \tau_{12}^{-1} + e_{12}},$$

$$p_2 = \frac{-Y_1(N_D + p)p_l^2 + (p_l[X_1 + X_{12}) + e_{12}](N_A - N_D - p)}{p_l(X_1 + X_{12} + Y_{21}) + \tau_{12}^{-1} + e_{12}},$$

$$p = p_l\frac{\alpha^3 + N_D\tilde{f}_r}{\alpha^3 N_l - \tilde{f}_r p_l}. \tag{51}$$

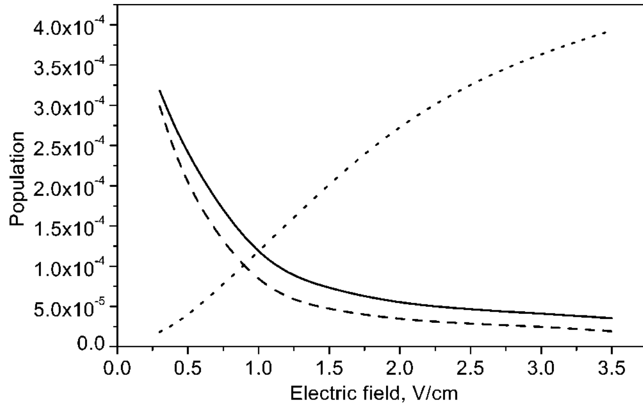

FIG. 5. Electric field dependencies of populations of the localized $1s$ (dashed line), $2p1$ (solid line), and resonant (dot line) states at $P=4$ kbar.

Thus, at given value of the electric field, the population functions $\tilde{f}^l_{\mathbf{k}}, \tilde{f}^l_{\mathbf{k}}$ are obtained as a solution to the system of Boltzmann equations (17). Then, the GR coefficients are calculated using the light hole population function $\tilde{f}^l_{\mathbf{k}}$. Finally, Eq. (50) should be solved to obtain light hole concentration and, then, the populations of the localized states should be found from Eq. (28).

One should notice here, that at certain values of the electric field, Eq. (50) may have multiple solutions. It results in S-type I-V characteristics of p-Ge in the impurity breakdown regime. This question for unstrained p-Ge was investigated in Ref. 28. The specific feature of this regime is that the population inversion between the excited and ground localized states, i.e., $f_{2p1} > f_{1s}$, could be achieved.

Figure 5 shows calculated electric field dependencies of the localized and the resonant states populations at $P=4$ kbar applied along [001] axis. One can see that the population of the localized states decreases with increasing of the electric field while the resonant state population increases. Starting from the electric field approximately equal to 1 V/cm intracenter population is realized. However, optical gain at frequency corresponding to the transition between the resonant and the excited localized state appears only if the gain due to the intracenter transition is larger than intravalence band absorption at the corresponding energy. This absorption plays the role of internal loses in the system. Other absorption mechanisms will be discussed below. At this point, we can conclude that the net THz gain may be realized at electric field stronger than 1 V/cm.

V. THZ GAIN

The experimental study of the stimulated emission from strained p-Ge was accomplished in Refs. 20 and 21. Analysis of the experiments showed that the strongest optical transition takes place between the $(1s,\text{res})$ and $2p1$ localized states. The energy of quantum corresponding to such transition measured at stress value of 4 kbar equals to 10 meV provided that the stress is applied along [111] direction. However, the energy of the quantum derived from the variational calculations of the binding energies of $(1s,\text{res})$ and $2p1$ localized states at the same value of stress has a value of 21 meV (see Table I). The main reason for such a discrepancy is the central cell potential effect which leads to an increase of the energy of s-type states having maximum of their wave functions at the impurity site. For example, the experimental value of the binding energy of Ga impurity in unstrained Ge is 1.5 meV higher than the value given by the effective mass theory. The resonant acceptor states induced by a short range potential were studied in Ref. 36. It was shown, that in opposite to the case of the resonant state induced by the Coulomb potential, the resonant state induced by the short range potential does not become attached to the heavy hole band. Instead, it is located in the middle of the energy gap between the light and the heavy hole bands and, therefore, its binding energy increases with increasing of the stress. This shows that one can expect much stronger effect of the short range part of the total impurity potential on the lowest resonant state binding energy than on the localized acceptor states. In this paper for calculation of the gain spectrum we take the value of $(1s,\text{res})$ resonant state binding energy equal to 12 meV to fit the experimentally measured value of the energy of the quantum for the above discussed optical transition, because the exact value of the energy of quantum determines the value of absorption, and correspondingly, the value of the net gain.

To calculate gain in the THz frequency range, optical transitions between the states of the light and heavy hole bands, between the light hole band states and the localized acceptor states, as well as between the resonant states and localized acceptor states will be considered. All these optical transitions can be considered as the intravalence band transitions. Gain coefficient $g(\hbar\omega)$ will be a sum of the gain coefficients due to the intravalence band transitions with the given energy $\hbar\omega$

$$g(\hbar\omega) = g_{hl}(\hbar\omega) + g_{l,1s}(\hbar\omega) + g_{l,2p1}(\hbar\omega), \tag{52}$$

where $g_{hl}(\hbar\omega)$ is the gain coefficient for the heavy-to-light hole optical transitions, $g_{l,1s}(\hbar\omega)$ and $g_{l,2p1}(\hbar\omega)$ are the gain due to the optical transitions between the light hole states and $1s$ and $2p1$ levels, correspondingly. The gain coefficient for the heavy-to-light hole transitions is given by[34,35]

$$g_{hl}(\hbar\omega) = \frac{4\pi^2}{n_r m_0^2 \omega c}\frac{1}{V}\sum_{\substack{\mathbf{k},\\ m=\pm 3/2,\\ m'=\pm 1/2}} |\langle l,\mathbf{k},m'|\mathbf{e}\cdot\hat{\mathbf{k}}|h,\mathbf{k},m\rangle|^2 \times (f^{h,m}_{\mathbf{k}} - f^{l,m'}_{\mathbf{k}}) \times \delta(\varepsilon^h_{\mathbf{k}} - \varepsilon^l_{\mathbf{k}} - \hbar\omega), \tag{53}$$

where c is the speed of light, m_0 is the free electron mass, n_r is the refractive index, and $\mathbf{e}$ is the polarization vector. Matrix elements of the operator $\mathbf{e}\cdot\hat{\mathbf{k}}$ in the Γ_8 basis can be obtained from the Luttinger Hamiltonian Eq. (1) for unstrained semiconductors by replacing $\hat{k}_i\hat{k}_j$ with the following combinations:

$$\hat{k}_i^2 \rightarrow (e_i\hat{k}_i),$$

$$\hat{k}_i\hat{k}_j \rightarrow (e_i\hat{k}_j + \hat{k}_i e_j). \tag{54}$$

Calculation of the light and heavy hole distribution functions in the presence of the external electric field performed in Sec. III did not reveal population inversion between the light and heavy hole band states corresponding to the same **k**. It means, that the value of g_{hl} should be negative and it gives the magnitude of the intravalence band absorption. The corresponding optical transitions are the mechanism of losses. Another mechanisms of losses might be indirect phonon or impurity assisted optical transitions which occur within the light or heavy hole bands. Calculation of the absorption coefficient due to such transitions should be done within the second order of the perturbation theory. In what follows, we will first calculate the value of the THz gain due to first order transitions and then compare the obtained result with the estimated value of the absorption coefficient due to the second order transitions.

Expressions for $g_{l,1s}(\hbar\omega)$ and $g_{l,2p1}(\hbar\omega)$ are similar to Eq. (53):

$$g_{l,1s(2p1)}(\hbar\omega) = \frac{4\pi^2}{n_r m_0^2 \omega c}\frac{1}{V}\sum_{\substack{\mathbf{k},\nu,\\ m=\pm 1/2,\\ m'=\pm 1/2}} |\langle 1s(2p1),\nu,m'|\mathbf{e}\hat{\mathbf{k}}|l,m,\mathbf{k}\rangle|^2 \times (f_{\mathbf{k}}^{l,m} - f_{1s(2p1),\nu}^{m'}) \times \delta(\varepsilon_{\mathbf{k}}^{l} - \varepsilon_{1s(2p1)} - \hbar\omega), \tag{55}$$

where ν denotes degenerated localized states in respect to the orbital angular momentum. In the presence of the resonant states, one should take $\Psi_{\mathbf{k}}^{m}(\mathbf{r})$ defined by Eq. (9) as the wave function of the light hole band states $|l,m,\mathbf{k}\rangle$. This wave function contains contributions from the localized states $\phi_{1s,\text{res}}^{m}$ at energies $\varepsilon_{\mathbf{k}}^{l}$ close to the resonance energy E_0 and scattered wave, which can be combined with the plane wave. When the energy of a light hole is far from E_0, $\Psi_{\mathbf{k}}^{m}(\mathbf{r})$ is reduced to the light hole band states wave function, which is perturbed only by the elastic Coulomb scattering. Thus, the matrix elements in Eq. (55) will consist of two terms, which can be attributed to "band-to-impurity" and "impurity-to-impurity" types of optical transitions. One should notice here, that for the transition to $1s$ localized state, only the first "planewave-like" term in Eq. (9) gives nonzero contribution to the matrix element. Contributions from the localized part and scattered wave vanish due to the selection rule in respect to parity. As wave functions of the localized $1s$ and $2p1$ states we adopt the variational functions given by Eqs. (7) and (8). In this work, we are interested only in relation of the strongest spectral line observed by Altukhov *et al.* with the spectral regions characterized by the positive value of the gain coefficient. Therefore the optical transitions between the resonant and the other excited localized acceptor states are excluded from the consideration.

The results of the calculations of the THz gain are shown in Fig. 6. One can find two regions of positive gain value. The main peak at the higher energy corresponds to the intracenter transitions from the lowest $(1s,\text{res})$ resonant state into $2p1$ excited localized state of the same impurity. The frequency of this peak does not depend on the electric field strength. The peak at longer wavelength is related to the band-to-impurity transitions and moves towards the higher energies with electric field getting stronger, because the distribution function maximum also moves to the higher energy region reflecting hole heating effect. The main peak in the gain spectrum corresponds to the main peak in the spectrum of stimulated emission measured in Ref. 20. However, no spectral lines in the low-energy spectral region were observed in these experiments. One possible reason is that the low energy spectral region does not fall into the sensitivity band of the detector used in these works.

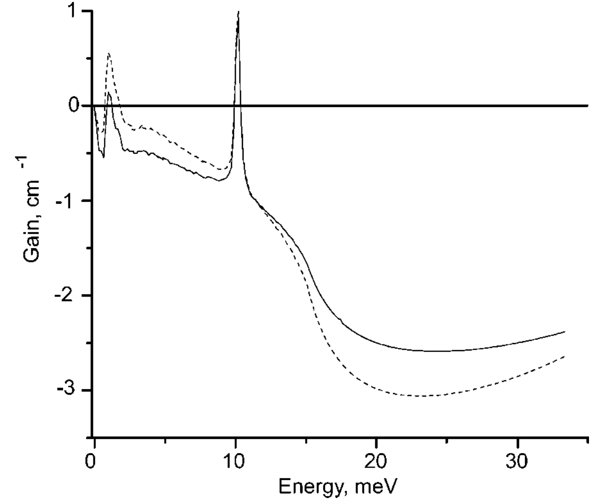

FIG. 6. Gain spectra for electric field strength 2 V/cm (solid line) and 3 V/cm (dashed line). The stress applied is 4 kbar.

Thus, the calculations show that the positive net THz gain due to the optical transitions between the $(1s,\text{res})$ and $2p1$ localized states of acceptors in strained p-Ge can be realized at stress value of 4 kbar. The magnitude of the gain is about 1 cm^{-1}. However, to make the final conclusion about the possibility of THz stimulated emission due to the intraimpurity optical transitions in strained p-Ge doped with boron acceptors, we should compare the value of the calculated THz gain with the values of other loss mechanisms. As we discussed above, the other possible loss mechanisms include intravalence band absorption due indirect phonon or impurity assisted transitions. The value of the absorption coefficients due to such transitions can be calculated by using the expression[37]

$$\alpha_{\text{loss}}(\omega) = \frac{n_r \omega_p^2 \gamma_s}{c(\omega^2 + \gamma_s^2)}, \tag{56}$$

where $\omega_p = 4\pi p_l e^2/(m_l n_r^2)$ is the plasma frequency, which corresponds to the carrier concentration p_l in the light hole band, m_l is an approximation for the light hole effective mass, and γ_s is the reverse scattering time of light holes due to interaction with acoustic phonons or ionized impurities. As a value of the light hole effective mass, we will take the density of states effective mass given by Eq. (30). The scat-

tering probabilities due to the interaction with acoustic phonons and ionized impurities were calculated in Sec. III and do not exceed values of $\gamma_s = 10^{11}$ s^{-1}. To get an estimation of plasma frequency, we take the concentration of the light holes equal to that of acceptor impurities. Thus, the value of the plasma frequency is $\omega_p = 5 \times 10^{11}$ s^{-1}. Finally, we obtain $\alpha_{\text{loss}} = 0.013$ cm^{-1} as the maximum value of the absorption coefficient due to the second order indirect transitions at the energy of quantum $\hbar\omega = 10$ meV corresponding to that of the intracenter $(1s, \text{res-}2p1)$ transition. This value is much smaller than the gain due to the first order intra impurity optical transitions (see Fig. 6), therefore the corresponding mechanisms of losses can be excluded from the consideration. Another possible mechanism of losses is the direct lattice absorption. However, in nonpolar crystals such as Ge, the value of the lattice absorption at the frequency of 2.5 THz is much less than 1 cm^{-1} and, therefore, can be neglected.[38]

The value of the THz gain due to the intracenter optical transition between the resonant and the excited localized acceptor states in strained p-Ge is much larger than that realized in p-Ge THz lasers operating under the external crossed electric and magnetic fields.[7] The cavity losses in both types of lasers have similar values due to similarity in cavity design, which utilizes the total internal reflection of the radiation propagating inside the sample.[20] Because of this, the quality factor of the cavity has the value of about 3000–5000 and emitted THz power is mostly limited by the effect of gain saturation rather than by the cavity losses.

The width of the gain peak shown in Fig. 6 equals to 0.8 meV and originates from the broadening of the resonant $(1s, \text{res})$ states due to hybridization with the light hole band states. The calculated value of the line width compares well with that observed in Ref. 20. Another possible broadening mechanism is due to the interaction of a hole captured into the resonant state with an acoustic phonon. However, our calculations show that the major contribution to the resonant state life time comes from the hybridization with the band states. The broadening may also come from the Coulomb interaction between the holes localized on neighboring impurities. For the impurity concentration used in this work, the average distance between the impurities is in the micrometer range while the characteristic width of the localized state wave function is of the order of 100 Å. This shows that the broadening due to inter impurity interaction can also be neglected when analyzing the spectral linewidth of the THz stimulated emission observed in Ref. 20. The above described analysis unambiguously shows that the gain at THz frequencies due to intraimpurity optical transitions between the resonant and localized states in strained p-Ge was achieved in the experiments described in the work of Altukhov *et al.*

VI. CONCLUSION

We have produced a comprehensive theoretical study of operation of strained p-Ge RSL. Kinetics of holes in strained p-Ge under an applied electric field has been studied and heavy and light hole distribution functions have been found. Nonequilibrium population of the localized acceptor states was obtained as a solution to the system of rate equations within the two-level model for impurity level structure. Conditions for the formation of the intracenter population inversion have been studied as a function of the electric field and external strain. We have observed that the population inversion is formed in a wide range of the electric field values and, therefore, could be easily achieved. The net gain from the sample at the THz frequencies was calculated using the nonequilibrium hole distribution function and the localized states population. The possibility to achieve net THz gain in semiconductors by injection of nonequilibrium carriers into impurity resonant state has been demonstrated. Peak THz gain has been calculated for different values of the electric field and strain.

ACKNOWLEDGMENTS

This work was supported by grants of The Swedish Foundation for Strategic Research, The Swedish Research Council (Grant No. TFR-THZ 2000-403), NorFA (Grant No. 000384), ISTC (Grant No. 2206), CRDF (Proposal No. 12655—"Resonant States and THz Emission in Semiconductor"), INTAS Grant No. YSF 2002-95, The Russian Foundation for Basic Research, The Russian Academy of Science, Russian Ministry of Science and Russian Scientific School (Grant No. 2192.2003.2).

APPENDIX A: ACCEPTOR RESONANT STATES

Here we present expressions for the quantities, which have appeared in Eq. (10) for the scattering and capture amplitudes

$$A_{\mathbf{k}}^{+1/2,+3/2} = V_{\mathbf{k}} \frac{b_{\mathbf{k}}}{N_{l\mathbf{k}}} - \frac{1}{V} \sum_{\mathbf{k}'} \frac{b_{\mathbf{k}'} \tilde{V}_{\mathbf{k}'\mathbf{k}}^{+1/2,+1/2} + c_{\mathbf{k}'} \tilde{V}_{\mathbf{k}'\cdot\mathbf{k}}^{-1/2,+1/2}}{N_{l\mathbf{k}'}} W_{\mathbf{k}'},$$

$$A_{\mathbf{k}}^{+1/2,-3/2} = V_{\mathbf{k}} \frac{c_{\mathbf{k}}^*}{N_{l\mathbf{k}}} - \frac{1}{V} \sum_{\mathbf{k}'} \frac{c_{\mathbf{k}'}^* \tilde{V}_{\mathbf{k}'\cdot\mathbf{k}}^{+1/2,+1/2} - b_{\mathbf{k}'}^* \tilde{V}_{\mathbf{k}'\cdot\mathbf{k}}^{-1/2,+1/2}}{N_{l\mathbf{k}'}} W_{\mathbf{k}'}, \tag{A1}$$

where

$$V_{\mathbf{k}} = \langle \varphi_{1s,\text{res}}(\mathbf{r}) | V_c(\mathbf{r}) | e^{i\mathbf{k}\cdot\mathbf{r}} \rangle = \frac{4\sqrt{\pi a_{\text{res}}^2 b_{\text{res}}} e^2}{\kappa a_{\text{res}}} V_1(k_z b_{\text{res}}, k_\perp a_{\text{res}}),$$

$$V_1(k_z b_{\text{res}}, k_\perp a_{\text{res}}) = \int_0^\infty r e^{-r} dr \int_0^1 \times \frac{\cos(b_{\text{res}} k_z r t) J_0(a_{\text{res}} k_\perp r \sqrt{1-t^2})}{\sqrt{1 - t^2\left(1 - \frac{b_{\text{res}}^2}{a_{\text{res}}^2}\right)}} dt,$$

$$W_{\mathbf{k}} = \langle \varphi_{1s,\text{res}}(\mathbf{r}) | e^{i\mathbf{k}\cdot\mathbf{r}} \rangle \frac{8\sqrt{\pi a_{\text{res}}^2 b_{\text{res}}}}{[1 + (k_z b_{\text{res}})^2 + (k_\perp a_{\text{res}})^2]^2},$$

$$\widetilde{V}_{\mathbf{k}'\cdot\mathbf{k}}^{-1/2,+1/2} = V_{\mathbf{k}'\cdot\mathbf{k}} \frac{b_{\mathbf{k}} c_{\mathbf{k}'}^{*} - b_{\mathbf{k}'} c_{\mathbf{k}}^{*}}{N_{l\mathbf{k}'} N_{l\mathbf{k}}},$$

$$\widetilde{V}_{\mathbf{k}'\cdot\mathbf{k}}^{+1/2,+1/2} = V_{\mathbf{k}'\cdot\mathbf{k}} \frac{b_{\mathbf{k}} b_{\mathbf{k}'}^{*} + c_{\mathbf{k}}^{*} c_{\mathbf{k}'} + d_{+\mathbf{k}}^{l} d_{+\mathbf{k}'}^{l}}{N_{l\mathbf{k}'} N_{l\mathbf{k}}},$$

$$V_{\mathbf{k}'\cdot\mathbf{k}} = \langle e^{-i\mathbf{k}'\cdot\mathbf{r}} | V_c(\mathbf{r}) | e^{i\mathbf{k}\cdot\mathbf{r}} \rangle = \frac{4\pi e^2}{\kappa(|\mathbf{k}' - \mathbf{k}|^2 + q_s^2)}, \qquad \text{(A2)}$$

where

$$q_s = (k_b T \kappa / 4\pi p e^2)^{-1/2} \qquad \text{(A3)}$$

is the screening wave vector, and k_b is the Boltzmann constant. The first terms in the expressions given by Eq. (11) for the scattering amplitudes, describe the scattering due to Coulomb interaction with ionized impurities in the Born approximation and the second terms describe the resonant scattering. Expressions for the energy level shift $\Delta E_{\mathbf{k}}$ and resonance width $\Gamma_{\mathbf{k}}$ are given by

$$\Delta E = -\frac{1}{8\pi^3} \int d^3\mathbf{k}' \frac{\left(\frac{\hbar^2}{2m_0} d_+(\mathbf{k}') - \Delta E\right) \frac{\hbar^2}{2m_0} d_-(\mathbf{k}')}{\frac{\hbar^2}{2m_0}[a_+(\mathbf{k}') + a_-(\mathbf{k}')] + 2\varepsilon_{\mathbf{k}'}} W_{\mathbf{k}'}{}^2 - \frac{1}{8\pi^3} P \int d^3\mathbf{k}' \frac{\left(\frac{\hbar^2}{2m_0} d_+(\mathbf{k}') - \Delta E\right) \frac{\hbar^2}{2m_0} d_-(\mathbf{k}')}{\frac{\hbar^2}{2m_0}[a_+(\mathbf{k}') + a_-(\mathbf{k}')] + 2\varepsilon_{\mathbf{k}'}} \times \frac{W_{\mathbf{k}'} V_{\mathbf{k}'}}{\varepsilon_{1s,\mathrm{res}} - E_{\mathrm{def}} + \Delta E - \varepsilon_{\mathbf{k}'}},$$

$$\frac{\Gamma}{2} = -\frac{1}{8\pi^2} \int d^3\mathbf{k}' \frac{\left(\frac{\hbar^2}{2m_0} d_+(\mathbf{k}') - \Delta e\right) \frac{\hbar^2}{2m_0} d_-(\mathbf{k}')}{\frac{\hbar^2}{2m_0}[a_+(\mathbf{k}') + a_-(\mathbf{k}')] + 2\varepsilon_{\mathbf{k}'}} \times W_{\mathbf{k}'} V_{\mathbf{k}'} \delta(\varepsilon_{\mathbf{k}'} + E_{\mathrm{def}} - \varepsilon_{1s,\mathrm{res}} - \Delta E).$$

APPENDIX B: SCATTERING PROBABILITIES

The theory of scattering by acoustic and optical phonons in strained semiconductors was formulated by Bir and Pikus,[33] and their results will be used here. The transition probability per unit time from the $\mathbf{k}$ Bloch state in the λ band to the $\mathbf{k}'$ Bloch state in the λ' band accompanied by the emission or absorption of acoustic phonon of frequency $\omega_{\mathbf{q},\nu}$ is given by

$$W_{\lambda\mathbf{k},\lambda'\mathbf{k}'}^{\mathrm{ac},\pm} = \frac{\pi}{\hbar} \sum_{\mathbf{q},\nu} \left(\frac{\hbar\left(n_{\mathbf{q},\nu} + \frac{1}{2} \pm \frac{1}{2}\right)}{2\rho\omega_{\mathbf{q},\nu} V} \right) \times \sum_{m,m'} |\langle \lambda' m' \mathbf{k}' | H^{\mathrm{ac}}(\mathbf{q}\nu) | \lambda m \mathbf{k} \rangle|^2 \times \delta_{\mathbf{q},\pm(\mathbf{k}-\mathbf{k}')} \delta(\varepsilon_{\mathbf{k}'}^{\lambda'} - \varepsilon_{\mathbf{k}}^{\lambda} \pm \hbar\omega_{\mathbf{q},\nu}), \qquad \text{(B1)}$$

where ρ is the mass density of the system, $\mathbf{q}$ is the phonon wave vector, ν the polarization, and $n_{\mathbf{q},\nu}$ is the number of phonons. In the sum, $m = \pm 1/2$ denotes the degenerated light hole band states ($\lambda, \lambda' = l$), and $m = \pm 3/2$ does the same for the degenerated heavy hole band states ($\lambda, \lambda' = h$). The sign "+" corresponds to the emission and "–" to the absorption of acoustic phonons. The explicit matrix form of the electron-acoustic phonon interaction Hamiltonian $H^{\mathrm{ac}}(\mathbf{q}\nu)$ can be found in Ref. 23.

Similarly, for the scattering by optical phonons, the transition probability per unit time has the form[33]

$$W_{\lambda\mathbf{k},\lambda'\mathbf{k}'}^{\mathrm{opt}} = \frac{\pi}{\hbar} \left(\frac{\hbar}{2\rho\omega_{\mathrm{opt}} V} \right) \sum_{s,m,m'} |\langle \lambda' m' \mathbf{k}' | H^{\mathrm{opt}}(\mathbf{e}_s) | \lambda m \mathbf{k} \rangle|^2 \delta(\varepsilon_{\mathbf{k}'}^{\lambda'} - \varepsilon_{\mathbf{k}}^{\lambda} - \hbar\omega_{\mathrm{opt}}), \qquad \text{(B2)}$$

where $\mathbf{e}_s$ is the polarization vector. Again, the expression of the electron-optical phonon interaction Hamiltonian $H^{\mathrm{opt}}(\mathbf{e}_s)$ is given in Ref. 33.

APPENDIX C: IMPACT IONIZATION PROBABILITIES

The probability of impact ionization from an impurity level n to a Bloch state $\mathbf{k}$ is given by

$$W_{\mathbf{k},n}^{i} = \frac{2\pi}{\hbar} \sum_{\mathbf{k}',\mathbf{k}''} |M_{\mathbf{k},\mathbf{k}',\mathbf{k}''}|^2 \delta(\varepsilon_{\mathbf{k}} - |\varepsilon_n| - \varepsilon_{\mathbf{k}'} - \varepsilon_{\mathbf{k}''}), \qquad \text{(C1)}$$

where

$$M_{\mathbf{k},\mathbf{k}',\mathbf{k}''} = \langle \mathbf{k}'', \mathbf{k}' | \hat{V}_c(\mathbf{r}_1 - \mathbf{r}_2) | n, \mathbf{k} \rangle, \qquad \text{(C2)}$$

and $\hat{V}(\mathbf{r}_1 - \mathbf{r}_2)$ is the operator of the screened Coulomb interaction between two holes. Calculation of the matrix element in Eq. (C2) gives

$$M_{\mathbf{k},\mathbf{k}',\mathbf{k}''} 8 \sqrt{\frac{\pi a_B^3 n^3}{V}} \frac{4\pi e^2}{\kappa} \frac{1}{V} \frac{1}{(|\mathbf{k}' - \mathbf{k}|^2 + q_s^2)} \times \frac{1}{(1 + a_B^2 n^2 |\mathbf{k}' - \mathbf{k} + \mathbf{k}''|^2)^2}. \qquad \text{(C3)}$$

Now we substitute Eq. (C3) into Eq. (C1) and integrate over polar angles of the momenta $\mathbf{k}''$ and $\mathbf{k}'$, thus introducing the function $\mathcal{J}(\varepsilon_{\mathbf{k}}, \varepsilon', \varepsilon'')$

$$\mathcal{J}(\varepsilon_{\mathbf{k}},\varepsilon',\varepsilon'') = \int_0^\pi d\theta' \frac{\sin\theta'}{(q_s^2a_B^2 + a_B^2|\mathbf{k}'-\mathbf{k}|^2)^2} \times \int_0^\pi d\theta'' \frac{\sin\theta''}{(1+a_B^2n^2|\mathbf{k}'-\mathbf{k}+\mathbf{k}''|^2)^4} = \int_{-1}^{1} \frac{dx'}{[q_s^2a_B^2+\phi(x')]^2}\frac{1}{3B}\frac{(A+B)^3-(A-B)^3}{(A+B)^3(A-B)^3}, \tag{C4}$$

where

$$\phi(x') = \varepsilon' + \frac{\varepsilon_{\mathbf{k}}}{E_B} - 2\sqrt{\varepsilon'\frac{\varepsilon_{\mathbf{k}}}{E_B}}x',$$

$$A = 1 + n^2[\varepsilon'' + \phi(x')],$$

$$B = 2n^2\sqrt{\varepsilon''}\sqrt{\phi(x')}. \tag{C5}$$

Integrating over energies, one can get

$$W^i_{\mathbf{k},n} = 32\frac{a_B^3n^3}{V}\frac{E_B}{\hbar}\mathcal{I}_1\left(\frac{\varepsilon_{\mathbf{k}}}{E_B}\right), \tag{C6}$$

where

$$\mathcal{I}_1\left(\frac{\varepsilon_{\mathbf{k}}}{E_B}\right) = \int_0^{\varepsilon_{\mathbf{k}}/E_B - 1/n^2} \sqrt{\varepsilon'}\sqrt{\varepsilon''}\mathcal{J}(\varepsilon_{\mathbf{k}},\varepsilon',\varepsilon'')d\varepsilon',$$

$$\varepsilon'' = \frac{\varepsilon_{\mathbf{k}}}{E_B} - \frac{1}{n^2} - \varepsilon'. \tag{C7}$$

Substituting Eq. (C6) into Eq. (37) and integrating over the energy $\varepsilon_{\mathbf{k}}$, the final expression for the impact ionization coefficient X_n is obtained in the form given by Eq. (41).

The probability of impact ionization from a localized impurity level n_1 to a localized impurity level level n_2 is given by

$$W^i_{\mathbf{k},n_1,n_2} = \frac{2\pi}{\hbar}g_{n_2}\sum_{\mathbf{k}'}|M_{\mathbf{k},\mathbf{k}',\mathbf{n}_1,\mathbf{n}_2}|^2\delta(\varepsilon_{\mathbf{k}} - |\varepsilon_{n_1}| - \varepsilon_{\mathbf{k}'} - |\varepsilon_{n_2}|), \tag{C8}$$

where the matrix element can be obtained in the form

$$M_{\mathbf{k},\mathbf{k}',\mathbf{n}_1,\mathbf{n}_2} = \langle n_2,\mathbf{k}'|\hat{V}_c(\mathbf{r}_1-\mathbf{r}_2)|n_1,\mathbf{k}\rangle = 8\frac{1}{V}\frac{\tilde{n}^3}{\sqrt{n_1^3n_2^3}}\frac{4\pi e^2}{\kappa}\frac{1}{(|\mathbf{k}'-\mathbf{k}|^2+q_s^2)} \times \frac{1}{(1+a_B^2\tilde{n}^2|\mathbf{k}'-\mathbf{k}|^2)^2},$$

$$\tilde{n}^{-1} = n_1^{-1} + n_2^{-1}, \tag{C9}$$

where g_{n_2} is the degeneracy factor of the level n_2. Integrating the matrix element in Eq. (C9) over polar angle of $\mathbf{k}'$, we introduce function $\mathcal{J}_1(\varepsilon_{\mathbf{k}}/E_B,\varepsilon')$

$$\mathcal{J}_1(\varepsilon_{\mathbf{k}},\varepsilon') = \int_0^\pi d\theta' \frac{\sin\theta'}{(q_s^2a_B^2+a_B^2|\mathbf{k}'-\mathbf{k}|^2)^2} \times \frac{1}{(1+a_B^2\tilde{n}^2|\mathbf{k}'-\mathbf{k}|^2)^4} = \int_{-1}^{1}\frac{dx'}{[q_s^2a_B^2+\phi(x')]^2}\frac{1}{[1+\tilde{n}\phi(x')]^2}. \tag{C10}$$

Substituting Eq. (C9) into Eq. (C8) and integrating over the energy $\varepsilon_{\mathbf{k}'}$ the following expression for $W^i_{\mathbf{k},n_1,n_2}$ is obtained

$$W^i_{\mathbf{k},n_1,n_2} = 2^{10}\pi g_{n_2}\frac{\tilde{n}^6}{n_1^3n_2^3}\frac{a_B^3}{V}\frac{E_B}{\hbar}\sqrt{\varepsilon'}\mathcal{J}_1\left(\frac{\varepsilon_{\mathbf{k}}}{E_B},\varepsilon'\right),$$

$$\varepsilon' = \frac{\varepsilon_{\mathbf{k}}}{E_B} - \frac{1}{n_1^2} - \frac{1}{n_2^2}. \tag{C11}$$

Substituting Eq. (C11) into Eq. (44) and integrating over the energy $\varepsilon_{\mathbf{k}}$, the final expression for the impact ionization coefficient X_{n_1,n_2} is obtained in the form of Eq. (46).

[1] R. E. Miles, in *Terahertz Sources and Systems*, edited by P. Harrison and D. Lippens, Vol. 27, NATO Science Series II (Kluwer, Dordrecht, 2001).
[2] P. Y. Han, G. C. Cho, and X.-C. Zhang, Opt. Lett. **25**, 242 (2000).
[3] D. M. Mittleman, R. H. Jacobsen, and M. C. Nuss, IEEE J. Sel. Top. Quantum Electron. **2**, 679 (1996).
[4] D. M. Mittleman, S. Hunsche, L. Boivin, and M. C. Nuss, Opt. Lett. **22**, 904 (1997).
[5] P. T. Lang, F. Sessler, U. Werling, and K. F. Renk, Appl. Phys. Lett. **55**, 2576 (1989).
[6] F. Lewen, S. P. Belov, F. Maiwald, T. Klaus, and G. Winnewisser, Z. Naturforsch., A: Phys. Sci. **50**, 1182 (1995).
[7] A. A. Andronov, Sov. Phys. Semicond. **21**, 701 (1987); Opt. Quantum Electron. **23** (1991).
[8] E. Bründermann, A. M. Linhart, H. P. Röser, O. D. Dubon, W. L. Hansen, and E. E. Haller, Appl. Phys. Lett. **68**, 1359 (1996); E. Bründermann, D. R. Chamberlin, and E. E. Haller, *ibid.* **73**, 2757 (1998).
[9] D. H. Auston, K. P. Cheung, and P. R. Smith, Appl. Phys. Lett. **45**, 284 (1984).
[10] B. B. Hu, X.-C. Zhang, and D. H. Auston, Phys. Rev. Lett. **67**, 2709 (1991).
[11] Y.-S. Lee, T. Meade, V. Perlin, H. Winful, T. B. Norris, and A. Galvanauskas, Appl. Phys. Lett. **76**, 2505 (2000).

[12] K. M. Evenson, D. A. Jennings, and F. R. Petersen, Appl. Phys. Lett. **44**, 576 (1984).

[13] S. Matsuura, M. Tani, and K. Sakai, Appl. Phys. Lett. **70**, 559 (1997).

[14] G. Dehlinger, L. Diehl, U. Gennser, H. Sigg, J. Faist, K. Ensslin, D. Gruntzmacher, and E. Muller, Science **290**, 2277 (2000).

[15] M. Rochat, J. Faist, M. Beck, U. Oesterle, and M. Ilegems, Appl. Phys. Lett. **73**, 3724 (1998).

[16] B. S. Williams, B. Xu, Q. Hu, and M. R. Melloch, Appl. Phys. Lett. **75**, 2927 (1999).

[17] J. Ulrich, R. Zobl, W. Schrenk, G. Strasser, and K. Unterrainer, Appl. Phys. Lett. **76**, 1928 (2000).

[18] M. Helm, P. England, E. Colas, F. De Rosa, and S. J. Allen, Phys. Rev. Lett. **63**, 74 (1989).

[19] R. Köhler, A. Tredicucci, F. Beltram, H. E. Beere, E. H. Linfield, A. G. Davies, D. A. Ritchie, R. C. Iotti, and F. Rossi, Nature (London) **417**, 156 (2002).

[20] I. V. Altukhov, E. G. Chirkova, M. S. Kagan, K. A. Korolev, V. P. Sinis, and F. A. Smirnov, Sov. Phys. JETP **74**, 404 (1992); I. V. Altukhov, E. G. Chirkova, M. S. Kagan, K. A. Korolev, V. P. Sinis, and I. N. Yassievich, Phys. Status Solidi B **198**, 35 (1996); I. V. Altukhov, M. S. Kagan, K. A. Korolev, V. P. Sinis, E. G. Chirkova, M. A. Odnoblyudov, and I. N. Yassievich, JETP **88**, 51 (1999).

[21] Yu. P. Gousev, I. V. Altukhov, K. A. Korolev, V. P. Sinis, and M. S. Kagan, Appl. Phys. Lett. **75**, 757 (1999).

[22] I. V. Altukhov, E. G. Chirkova, V. P. Sinis, M. S. Kagan, Yu. P. Gousev, S. G. Thomas, K. L. Wang, M. A. Odnoblyudov, and I. N. Yassievich, Appl. Phys. Lett. **79**, 3909 (2001).

[23] A. Blom, M. A. Odnoblyudov, H. H. Cheng, I. N. Yassievich, and K. A. Chao, Appl. Phys. Lett. **79**, 713 (2001).

[24] M. A. Odnoblyudov, I. N. Yassievich, V. M. Chistyakov, and K. A. Chao, Phys. Rev. B **62**, 2486 (2000).

[25] M. I. D'yakonov and A. V. Khaetski, Sov. Phys. JETP **59**, 1072 (1984).

[26] M. A. Odnoblyudov, A. A. Prokofiev, and I. N. Yassievich, JETP **94**, 593 (2002).

[27] M. A. Odnoblyudov, I. N. Yassievich, M. S. Kagan, and K. A. Chao, Phys. Rev. B **62**, 15 291 (2000).

[28] W. Quade, G. Hüpper, E. Schöll, and T. Kuhn, Phys. Rev. B **49**, 13 408 (1994).

[29] E. Schöll, *Nonequilibrium Phase Transitions in Semiconductors* (Springer, Berlin, 1987).

[30] V. N. Abakumov, V. I. Perel, and I. N. Yassievich, in *Modern Problems in Condensed Matter Sciences*, edited by V. M. Agranovich and A. A. Maradudin (North-Holland, Amsterdam, 1991).

[31] M. A. Odnoblyudov and V. M. Chistyakov, Semiconductors **32** 799 (1998).

[32] W. Kohn and J. M. Luttinger, Phys. Rev. **98**, 915 (1955).

[33] G. L. Bir and G. E. Pikus, *Symmetry and Strain Effects in Semiconductors* (Wiley, New York, 1974).

[34] Y.-C. Chang, R. B. James, Phys. Rev. B **39**, 12 672 (1989).

[35] J. Taylor, V. Tolstikhin, J. Appl. Phys. **87**, 1054 (2000).

[36] M. A. Odnoblyudov, A. A. Pakhomov, V. M. Chistyakov, and I. N. Yassievich, Fiz. Tekh. Poluprovodn. (S.-Peterburg) **31**, 1180 (1997) [Semiconductors **31**, 1014 (1997)].

[37] P. Y. Yu and M. Cardona, *Fundametals of Semiconductors: Physics and Materials Properties* (Springer, Berlin, 2001).

[38] A. Dargys and J. Kundrotas, *Handbook on Physical Properties of Ge, Si, GaAs and InP* (Science and Encyclopedia Publishers, Vilnus, 1994).